

# Highly Efficient Organic/Inorganic Hybrid Nonlinear Optic Materials via Sol–Gel Process: Synthesis, Optical Properties, and Photobleaching for Channel Waveguides

Hwan Kyu Kim\*

Department of Macromolecular Science, Hannam University, Taejon, Korea 306–791

Su-Jin Kang and Sam-Kwon Choi

Department of Chemistry, Korea Advanced Institute of Science & Technology,  
Taejon, Korea 305-701

Yu-Hong Min and Choon-Sup Yoon\*

Department of Physics, Korea Advanced Institute of Science & Technology,  
Taejon, Korea 305–701

Received September 18, 1998

The thermally stable second-order nonlinear optic (NLO) hybrid materials were successfully prepared by a sol–gel process using dye-attached sol–gel monomers (ormosils) of difunctionalized or trifunctionalized second-order NLO chromophores attached to silicon atoms. The dye-attached sol–gel monomers were synthesized by the coupling reaction of 3-isocyanatopropyltriethoxysilane with the corresponding functionalized NLO chromophores in DMAc. The dye-attached sol–gel monomers were homopolymerized and copolymerized with TEOS by hydrolysis and polycondensation in the presence of a slight excess amount of acidified water (pH 3), yielding the hybrid precursors (or a homogeneous solution). The hybrid precursors were spin-coated on various substrates such as ITO glass and NaCl disk. Hybrid films were further polycondensed by curing at 170 °C for 3 h. The cured hybrid materials existed in monohydroxy ( $T^2$ ,  $Q^3$ ) and nonhydroxy ( $T^3$ ,  $Q^4$ ) states, indicating the formation of a highly cross-linked silicon–oxygen polymeric network. All of the cured organic/SiO<sub>2</sub> hybrid films are transparent. The organic/SiO<sub>2</sub> hybrid materials were quite stable at elevated temperatures above 250 °C. The hybrid films were poled by corona discharge technique or dc contact electrode. The values of electro-optic coefficient for the organic/SiO<sub>2</sub> hybrid materials were in the range of 3.7 to 16 pm/V at the wavelength of 1.3 μm, depending on dye-attached sol–gel monomers and poling conditions. The SG-DANS (1:2:2) film shows excellent temporal stability. The  $r_{33}$  signal remained at 80% of its initial value after heating even at 150 °C for 3 h. Also, the second-order nonlinear optical coefficient  $d_{31}$  of 72 pm/V for the SG-DANS (1:2:0) hybrid film measured by the Maker fringe technique was obtained. The refractive index was decreased after photobleaching. Using the hybrid film, a single-mode channel waveguide was also fabricated by the photobleaching method. The mode pattern confirmed that a channel waveguide was single-mode, and the optical propagation loss was measured to be less than 1 dB/cm.

## Introduction

In recent years, poled nonlinear optic (NLO) polymers, where organic NLO chromophores with large molecular hyperpolarizability are covalently bonded to the polymer backbone, have been paid much attention for use in photonic applications such as high-speed photonic switching devices and electro-optic modulators.<sup>1–5</sup> For practi-

cal applications, these NLO polymeric materials must exhibit properties such as high optical quality thin film formability, high optical damage thresholds, sufficiently large and stable NLO susceptibilities, low beam propagation loss and feasibility of device fabrication. Although it is extremely difficult to synthesize such materials which possess the material requirements for practical applications, numerous approaches have been developed to utilize these NLO polymeric materials for use in real applications.<sup>2,6</sup>

\* To whom all the correspondence should be addressed.

(1) Williams, D. J. *Nonlinear Optical Properties of Organic Materials*; ACS Symposium Series 253; American Chemical Society: Washington, DC, 1983.

(2) Williams, D. J. *Angew. Chem., Int. Ed. Engl.* **1984**, *23*, 690.

(3) Burland, D. M.; Miller, R. D.; Walsh, C. A. *Chem. Rev.* **1994**, *94*, 31.

(4) Becker, M.; Sapochak, L.; Ghosen, R.; Xu, C.; Dalton, L. R.; Shi, T.; Steier, W. H.; Jen, A. K. Y. *Chem. Mater.* **1994**, *6*, 104.

(5) Peng, Z.; Yu, L. *Macromolecules* **1994**, *27*, 2638. (b) Walsh, C. A.; Burland, D. M.; Lee, V. Y.; Miller, R. D.; Smith, B. A.; Twieg, R. J.; Volkson, W. *Macromolecules* **1993**, *26*, 3720.

(6) Jen, A. K. Y.; Drost, K. J.; Cai, Y.; Rao, V. P.; Dalton, L. R. *J. Chem. Soc., Chem. Commun.* **1994**, 965.

Recently, high glass transition temperature polymers such as aromatic polyimide<sup>7,8</sup> and aromatic polyesters<sup>9</sup> were developed as polymeric backbones for the purpose of restraining the relaxation of the noncentrosymmetric chromophore-alignment induced by an electric field. Among them, NLO functionalized aromatic polyimides have shown promising potential in device applications due to the higher temperature alignment stability and better mechanical properties and processability than other NLO polymeric systems, such as a side chain system and a guest–host NLO chromophore-polyimide system. However, most functionalized NLO polyimides were prepared from the corresponding polyamic acids via thermal treatments. It was reported that polyimides derived from polyamic acids exhibited poor reproducibility of optical quality, including high optical propagation loss and also decomposition of side NLO chromophores during the imidization process at a high curing temperature.<sup>4,10</sup> Their high optical loss still limits device applications.

Recently, we reported the development of polyamideimides containing NLO chromophores by the direct polycondensation of difunctionalized NLO chromophores with various aromatic dianhydrides, to enhance the stability of dipole alignment and their solubility.<sup>4,10</sup> We also noted that these side chain NLO polyamideimides have several advantages, including higher temperature alignment stability, better mechanical properties, and lower optical propagation loss than other polyimides derived from polyamic acids.

Very recently, in an effort to achieve a large second-order coefficient, good temporal stability, and low beam propagation loss, we employed organic/silica hybrid materials in which silica network is heavily cross-linked. The reason we chose the silica network as a polymer matrix was that there was a possibility that the SiO<sub>2</sub> network would possess high  $T_g$ , good optical transparency, good chemical endurance, and mechanical stability. The SiO<sub>2</sub> network can be easily synthesized by a sol–gel technique, and NLO chromophores are anchored to the silica network during low-temperature processing. This sol–gel process offers an attractive route to the preparation of a three-dimensional inorganic network with high-dimensional stability and excellent optical clarity, including a highly stable and large electro-optic (EO) property. The sol–gel process has some advantages such as the ease of film fabrication and high stability of dipole alignment by locking the chromophore in the silica networks (SiO<sub>2</sub>). A number of approaches have been reported on the nonlinear optic effects in poled organic/silica hybrid films. The early system studied by Zhang et al. was “host–guest” where the NLO chromophore was physically blended into the sol–gel matrix.<sup>11</sup> They achieved a moderate  $\chi^{(2)}$  value of 10.9 pm/

V, and 80% of this value remained after 3 months at room temperature. However, this system has the following problems: The solubility of guest molecules into the silica matrix is limited to under 15 wt %. At higher concentration of NLO organic dye, the phase segregation of the NLO dye is prone to happen during only the curing process. Phase separation between organic (NLO dye) and inorganic (SiO<sub>2</sub>) compounds, sublimation of a dye, and cracking of film are apt to occur during the poling/curing process. Kim et al. fabricated the “side chain” sol–gel film where the monofunctionalized NLO chromophore was attached to the Si atom.<sup>12</sup> The  $d_{33}$  value of 11 pm/V was obtained by the corona poling method, but the relaxation of the film has not been studied. Nosaka et al. prepared sol–gel-processed SiO<sub>2</sub> films where organic chromophores were both doped and attached.<sup>13</sup> In this experiment, the side chain system showed more enhanced temporal stability than the host–guest system. Recently, Yang et al. synthesized a sol–gel-processed film where the NLO chromophore was attached to the Si atom via three linkages.<sup>14</sup> They obtained 27 pm/V for the  $d_{33}$  value by the corona poling method and this film retained over 80% of its initial value after 500 h at 100 °C. Hayashi et al. also described thermally stable sol–gel-processed NLO materials where a high concentration of NLO chromophore was doped to sol–gel-processed silica networks.<sup>15</sup> They obtained 120 pm/V for the  $d_{33}$  value from a corona-poled film and the  $d_{33}$  value was stable up to 125 °C without any relaxation for 1000 h.

The main aim of our study is to investigate the synthesis and optical properties of sol–gel-derived organic/silica hybrid films more precisely and systematically. The chemical structure of synthesized NLO organic/inorganic hybrid materials was determined by FT-IR, UV–visible, and solid-state <sup>29</sup>Si MAS NMR spectroscopy. The second-order nonlinear coefficient and electro-optic coefficient were measured, and other optical and physical properties such as refractive index were determined. The hybrid films were poled by the corona discharge technique or dc contact electrode poling under different conditions. The stability and relaxation of the electro-optic coefficients for the hybrid films were studied by measurement of the electro-optic coefficient as a function of time and temperature. We also have interest in the application of the hybrid films to waveguide devices. Therefore, the photobleaching effect was studied as a function of exposure time with an intense UV light for the fabrication of a single-mode channel waveguide. Preliminary results on the fabrication process and the beam propagation characteristics are also presented.

## Experimental Section

**Materials.** 3-Isocyanatopropyltriethoxysilane (IP-TriEOS; Lancaster Chemical Co.) and tetraethoxysilane (TEOS; Aldrich Chemical Co.) were used after distillation. *N,N*-Dimethyl-

(7) Kim, H. K.; Lee, H. J.; Lee, M. H.; Han, S. G.; Kim, H.-Y.; Kang, K. H.; Won, Y. H. *ACS Symp. Ser.* **1995**, *601*, 111.

(8) Lee, H. J.; Kang, S. J.; Kim, H. K.; Cho, H. N.; Park, J. T.; Choi, S. K. *Macromolecules* **1995**, *28*, 4638.

(9) Moy, T. M.; McGrath, J. E. *J. Polym. Sci., Part A: Polym. Chem.* **1994**, *32*, 1903.

(10) (a) Kim, H. K.; Moon, I. K.; Jin, M. Y.; Choi, K. Y. *Kor. Polym. J.* **1997**, *5*, 57. (b) Kim, H. K.; Moon, I. K.; Lee, H. J.; Kim, D.-J. *Mol. Cryst. & Liq. Cryst.* **1997**, *294*, 259. (c) Kim, H. K.; Moon, I. K.; Lee, H. J.; Han, S. G.; Won, Y. H. *Polymer* **1998**, *39*, 1719.

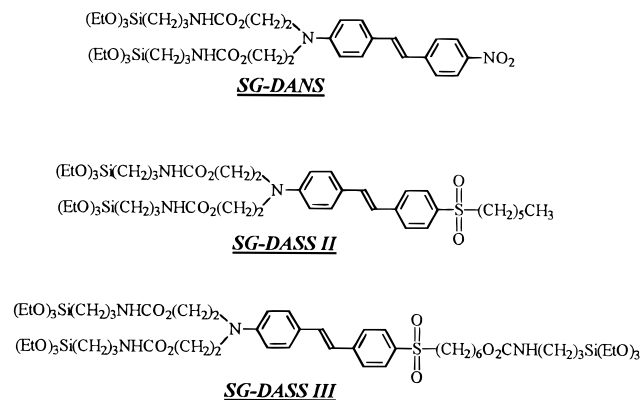
(11) Zhang, Y.; Prasad, P. N.; Burzynski, R.; *Chem. Mater.* **1992**, *4*, 851.

(12) Kim, J.; Plawsky, J. L.; LaPeruta, R.; Korenowski, G. M. *Chem. Mater.* **1992**, *4*, 249.

(13) Nosaka, Y.; Tohriwa, N.; Kobayashi, T.; Fujii, N. *Chem. Mater.* **1993**, *5*, 930.

(14) Yang, Z.; Xu, C.; Wu, B.; Dalton, L. R.; Kalluri, S.; Steier, W. H.; Shi, Y.; Bechtel, J. H. *Chem. Mater.* **1994**, *6*, 1899.

(15) Hayashi, H.; Nakayama, H.; Sugihara, O.; Okamoto, N. *Opt. Lett.* **1996**, *20*, 2264.

**Scheme 1. Chemical Structure of Dye-Attached Sol-Gel Monomers (Ormosils)**


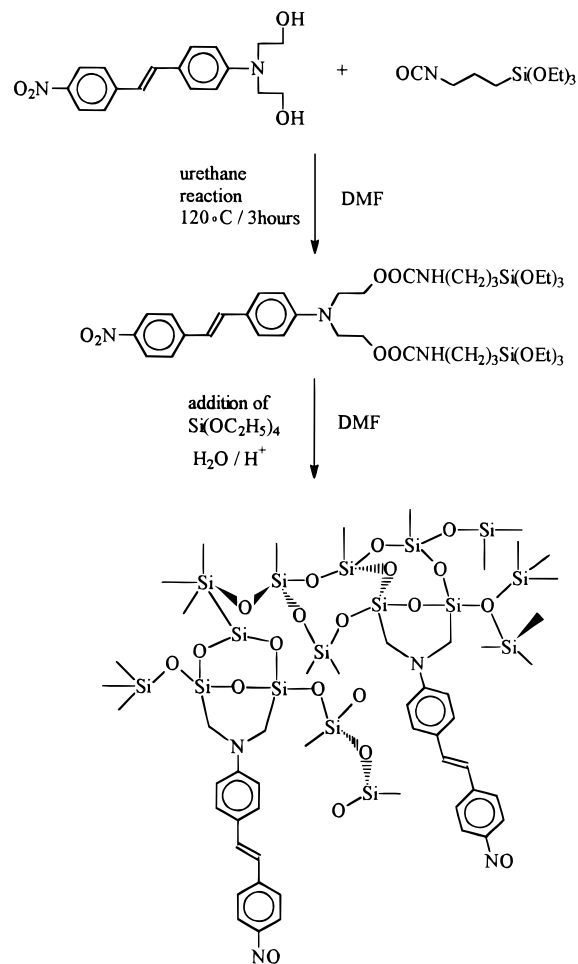
acetamide (DMAc) was dried over  $\text{MgSO}_4$  and distilled over  $\text{MgSO}_4$  under the reduced pressure. The various functionalized NLO stilbene derivatives of 4-[*N,N*-bis(2-hydroxyethyl)amino]-4'-nitrostilbene (DANS-diol), 4-[*N,N*-bis(2-hydroxyethyl)amino]-4'-hexylsulfonylstilbene (DASS-diol), and 4-[*N,N*-bis(2-hydroxyethyl)amino]-4'-(6-hydroxyethyl)sulfonylstilbene (DASS-triol) were synthesized via modified procedures of the cited references.<sup>8,10,16-19</sup> Different sol-gel monomers were synthesized by the coupling reactions of 3-isocyanatopropyltriethoxysilane with the various functionalized NLO stilbene derivatives in DMAc. Other chemical reagents were obtained from Aldrich Chemical Co. and used without further purification. Solvents were used after purification according to conventional methods.

**Synthesis of 4-[*N,N*-bis(2-(triethoxysilanoxyethylamino))-4'-nitrostilbene (SG-DANS).** The synthesis of DANS-diol was carried out in a cited reference (see Scheme 1).<sup>20</sup> The synthesis of 4-[*N,N*-bis(2-(triethoxysilanoxyethylamino))-4'-nitrostilbene (SG-DANS) was achieved as follows: DANS-diol (0.82 g,  $2.5 \times 10^{-3}$  mol) was placed in the flask and dissolved in the dry DMAc (20 mL). 3-Isocyanatopropyltriethoxysilane (1.2 g,  $5 \times 10^{-3}$  mol) was added to a flask. The reaction mixture was stirred for 6 h at 110 °C under a nitrogen atmosphere. This solution was used for the in situ sol-gel process. The sample for NMR analysis was obtained by precipitating the solution into hexane and dried under vacuum oven at 25 °C for 12 h. The peak of the isocyanato group is clearly absent in the monomer spectrum, and the new carbonyl peak at 1700  $\text{cm}^{-1}$  (urethane bond) appears.  $^1\text{H}$  NMR ( $\text{CDCl}_3$ ):  $\delta$  0.58 (t, 4H), 1.21 (t, 18H), 1.52 (m, 4H), 3.12 (t, 4H), 3.62 (t, 4H), 3.76 (q, 12H), 4.26 (t, 4H), 4.97 (t, 2H), 6.95–8.16 (m, 10H).  $^{13}\text{C}$  NMR ( $\text{CDCl}_3$ )  $\delta$  7.5 ( $\text{CH}_2\text{Si}$ ), 18.27 ( $\text{CH}_3\text{CH}_2\text{OSi}$ ), 23.1 ( $\text{CH}_2\text{CH}_2\text{Si}$ ), 43.4 ( $\text{NHCH}_2\text{CH}_2\text{CH}_2$ ), 50.9 ( $\text{NCH}_2\text{CH}_2\text{O}$ ), 58.4 ( $\text{CH}_3\text{CH}_2\text{OSi}$ ), 60.2 ( $\text{NCH}_2\text{CH}_2\text{O}$ ), 112.0, 112.4, 121.6, 121.9, 124.1, 126.1, 128.5, 133.4, 133.6, 145.0 (stilbene), 158 ( $\text{CO}_2\text{N}$ ).

In a similar way, 4-[*N,N*-bis(2-(triethoxysilanoxyethylamino))-4'-hexylsulfonylstilbene (SG-DASS II) and 4-[*N,N*-bis(2-(triethoxysilanoxyethylamino))-4'-(6-triethoxysilanoxyhexyl)sulfonylstilbene (SG-DASS III) were prepared (see Scheme 1).

**4-[*N,N*-Bis(2-(triethoxysilanoxyethylamino))-4'-hexylsulfonylstilbene (SG-DASS II):**  $^1\text{H}$  NMR ( $\text{CDCl}_3$ ):  $\delta$  0.58 (t, 4H), 1.21 (t, 18H), 1.52 (m, 4H), 3.12 (t, 4H), 3.62 (t, 4H), 3.72 (q, 12H), 0.83 (t, 3H), 1.23 (m, 6H), 1.67 (m, 2H), 3.05 (t, 2H), 3.20 (t, 4H), 3.85 (t, 2H), 6.90 (d, 2H), 6.98 (d, 1H), 7.21 (d, 1H), 7.43 (d, 2H), 7.56 (d, 2H), 7.82 (d, 2H).

**4-[*N,N*-Bis(2-(triethoxysilanoxyethylamino))-4'-(6-triethoxysilanoxyhexyl)sulfonylstilbene (SG-DASS III):**  $^1\text{H}$

**Scheme 2. A Schematic Route for Synthesizing Organic/Silica Hybrid Materials by the Sol-Gel Process**


NMR ( $\text{CDCl}_3$ ):  $\delta$  {0.58 (t, 6H), 1.21 (t, 27H), 1.52 (m, 6H), 3.12 (t, 6H), 3.76 (q, 18H)} from isocyanatopropyltriethoxysilane, 1.26–1.67 (m, 8H), 0.83 (t, 3H), 3.20 (t, 2H), 3.32 (t, 2H), 3.40 (t, 4H), 3.56 (t, 4H), 4.70 (d, 3H), 6.74 (d, 2H), 7.1 (d, 1H), 7.40 (d, 1H), 7.49 (d, 2H), 7.77 (m, 4H).  $^{13}\text{C}$  NMR ( $\text{CDCl}_3$ )  $\delta$  7.6 ( $\text{CH}_2\text{Si}$ ), 23.0 ( $\text{CH}_2\text{CH}_2\text{Si}$ ), 43.4 ( $\text{NHCH}_2\text{CH}_2\text{CH}_2$ ), 18.27 ( $\text{CH}_3\text{CH}_2\text{OSi}$ ), 58.4 ( $\text{CH}_3\text{CH}_2\text{OSi}$ ), 22.6, 27.8, 28.2 (methylene), 52.3 ( $\text{CH}_2\text{SO}_2$ ), 54.4 ( $\text{NCH}_2\text{CH}_2\text{O}$ ), 58.6 ( $\text{CH}_2\text{CH}_2\text{CH}_2\text{O}$ ), 60.2 ( $\text{NCH}_2\text{CH}_2\text{O}$ ), 111.5, 121.1, 123.5, 126.3, 128.2, 128.5, 132.8, 136.1, 143.5, 151.3 (stilbene), 156.0 ( $\text{CO}_2\text{N}$ ).

**Preparation of Hybrid Precursors (Sol) by the Sol-Gel Process.** The alkoxy silane containing the second-order NLO dye (SG-DANS or SG-DASS) was synthesized by the coupling reaction between an alcoholic NLO chromophore and 3-isocyanatopropyltriethoxysilane at 110 °C for 6 h in DMAc (10 mL) solvent. To the resulting solution was added tetraethylorthosilicate and then a slight excess amount of acidic water (pH 3). Various monomers were homopolymerized and copolymerized with TEOS. The solution was stirred for 3 days at room temperature, providing a homogeneous solution (or sol; a hybrid precursor). The viscosity of reaction solutions increased after the hydrolysis and polycondensation reaction. The sol-gel process is outlined in Scheme 2.

**Organic/SiO<sub>2</sub> Hybrid Film Preparation.** Every sol was applied to the substrate with a syringe through a Teflon membrane filter (Millipore, 0.22  $\mu\text{m}$  Millex-GS) until the substrate was completely covered. The sol was spin-coated on the ITO glass, a NaCl disk, and a silicon wafer for several measurements, such as electro-optic coefficient, UV-visible spectra, FT-IR, and determination of refractive indices. The film thickness was controlled by changing the viscosity of the sol by evaporating DMAc solvent from the sol solution. The

(16) Robello, D. R. *J. Polym. Sci. Part A: Polym. Chem.* **1990**, *28*, 1.

(17) Kang, S. J.; Lee, H. J.; Park, J. T.; Choi, S. K.; Kim, H. K. *Polym. Bull.* **1995**, *35*, 599.

(18) Demartino, R. N.; Yoon, H. N. U.S. Patent 4,808,332, 1989.

(19) Lee, H. J.; Won, Y. H.; Kang, S. J.; Choi, S. K.; Kim, H. K. *J. Polym. Sci. Part A: Polym. Chem.* **1996**, *34*, 2333.

(20) Lee, H. J.; Kim, H. K.; Lee, M. H.; Han, S. K.; Kim, H. Y.; Won, Y. H. *Polym. Bull.* **1996**, *36*, 279.



NLO chromophore-containing films were dried under vacuum oven for 6 h at room temperature to remove the residual solvent. The sol solution was converted into gel by removing the solvent from the sol solution, drying, and curing it for use in the thermal and solid-state  $^{29}\text{Si}$  NMR analyses.

**Measurement of the Refractive Index and Thickness.** The refractive index ( $n$ ) at the wavelength of  $1.3\ \mu\text{m}$  and the thickness ( $d$ ) of the hybrid films were measured by determining the propagation constants of at least the two lowest order transverse electric optical guided modes for samples cast on a glass substrate. The modes were excited with a diode laser beam that was prism-coupled into the film. Using the propagation constants, the mode equation for a three-layer waveguide was solved for  $n$  and  $d$ . The thickness was confirmed with an  $\alpha$ -step surface or depth profiler.

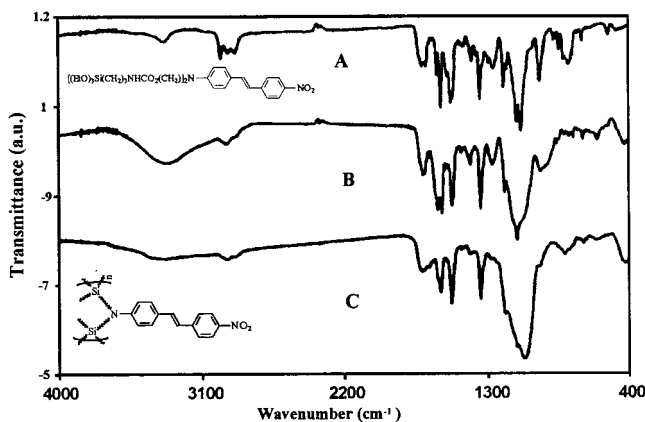
**Poling and Further Polymerization.** To establish the second-order nonlinear effect in the film, both corona poling and dc contact poling methods were employed. The hybrid precursor films spin-coated on indium tin oxide (ITO) glass were further thermally polycondensed and simultaneously poled using a corona discharge technique. The films were placed at a distance of 2 cm under the corona tip or wire, and a potential of 6–14 kV was applied. The poling process started at ambient temperature and then the sample temperature was increased at the rate of  $2\ ^\circ\text{C}/\text{min}$ . The films were heated to  $120\ ^\circ\text{C}$ , maintained at  $120\ ^\circ\text{C}$  for 3 h, then heated to  $170\ ^\circ\text{C}$ , and maintained at  $170\ ^\circ\text{C}$  for 3 h. After the poling process, the film temperature was reduced to ambient temperature and then the electric field was removed, yielding poled/cured hybrid films.

For dc contact poling, the films were soft baked at  $180\ ^\circ\text{C}$  for 20 min and then a gold electrode of 50 nm thickness was vacuum deposited on the film surface. At room temperature, dc voltage was applied across the film and the temperature was increased slowly. The film was kept at the elevated temperature of  $180\ ^\circ\text{C}$  for different times (see Table 2) and cooled to room temperature, while the dc voltage was maintained.

**Electrooptic Measurements.** Aluminum or gold electrode was evaporated on the top of the cured/poled hybrid film. The electro-optic coefficient,  $r_{33}$ , of the poled films was measured at the wavelength of  $1.3\ \mu\text{m}$  using a simple reflection method.<sup>21</sup> A Soleil-Babinet compensator was used to bias the dc intensity at the half-maximum intensity. The phase retardation between the p- and s-waves was modulated at about 170 Hz. The amplitude of the modulated intensity was determined using a lock-in amplifier, which can be used to calculate the  $r_{33}$  values.

## Results and Discussion

**Preparation of Organic/SiO<sub>2</sub> Hybrid Materials by the Sol-Gel Process.** Various dye-attached sol-gel monomers (ormosils) were synthesized by the coupling reaction of 3-isocyanatopropyltriethoxysilane with the corresponding functionalized NLO chromophores in dry DMAc, as shown in Scheme 1.<sup>20,22</sup> Their dye-attached sol-gel monomers were identified by FT-IR spectroscopy (see Figure 1). The resulting solution was actually used for an in situ sol-gel process. We have carried out the sol-gel process with a hydrochloric acid catalyst system, to prepare highly stable second-order NLO polymers. The sol-gel process for NLO organic/SiO<sub>2</sub> hybrid materials is outlined in Scheme 2. The dye-attached sol-gel monomer was homopolymerized and copolymerized with TEOS. To the resulting solution was added tetraethylorthosilicate and then a slight excess amount of acidic water (pH 3). With this synthetic



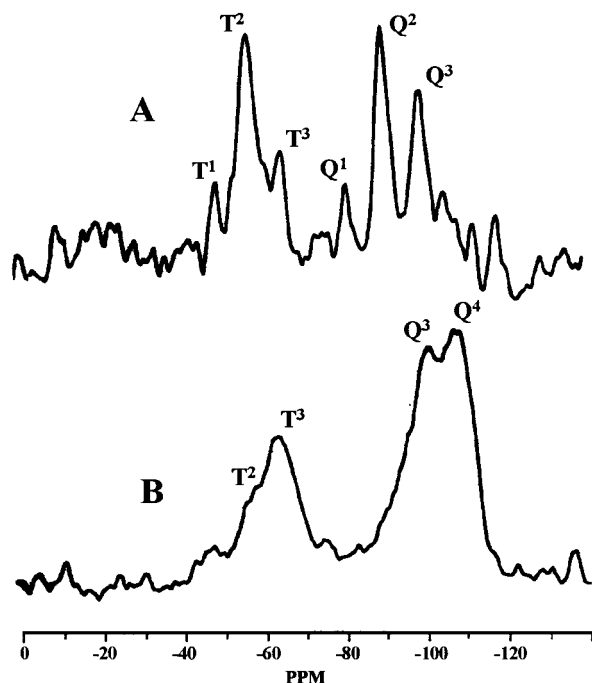
**Figure 1.** The FT-IR spectra of (a) a dye-attached sol-gel monomer, (b) a hybrid precursor (sol), and (c) an organic/SiO<sub>2</sub> hybrid material by the sol-gel process (SG-DANS (1:2:2)).

procedure, three kinds of hybrid films, which had a different molar ratio of DANS-diol, IP-TriEOS, and TEOS, were prepared. The molar ratios are noted in the parentheses (for example, SG-DANS (1:2:3)) when necessary. The addition of TEOS was intended to increase the cross-linking density to reduce the free volume of the silica matrix. The quantity of the HCl solution was such that the molar ratio of ethoxy group to H<sub>2</sub>O was about 1:0.6. The mixture was stirred at room temperature for several days. As hydrolysis and condensation reactions proceeded, the SiO<sub>2</sub> network was formed and the viscosity of the mixture increased gradually. When the appropriate viscosity was reached, the mixture was filtered through a  $0.22\ \mu\text{m}$  pore size syringe filter. Thin films were made by spin casting onto the clean ITO substrate. The film thickness was controlled by changing the viscosity of solution by evaporating DMAc solvent from the sol solution. The film thickness was in the range of  $1.83$ – $3.2\ \mu\text{m}$ , as measured by an  $\alpha$ -step surface or depth profiler. Furthermore, the films were converted into the gel state by drying the films. The films were further condensed and cured at  $170\ ^\circ\text{C}$  for 3 h, yielding organic/SiO<sub>2</sub> hybrid films with good optical quality. The organic/SiO<sub>2</sub> hybrid films had good adhesion to the ITO glass. When the cured samples were soaked in DMAc, which is a good solvent for the dye-attached sol-gel monomer, the solvent did not extract any measurable concentration of the dye from the films, indicating that the NLO dye is firmly incorporated in the silicon-oxygen network.

**Structural Characterization of Organic/SiO<sub>2</sub> Hybrid Materials.** The chemical structure of organic/SiO<sub>2</sub> hybrid materials was studied by FT-IR and  $^{29}\text{Si}$  NMR spectroscopy. Figure 1 shows the FT-IR spectra of a dye-attached sol-gel monomer, a hybrid precursor (sol), and an organic/SiO<sub>2</sub> hybrid material (SG-DANS (1:2:2)). The hybrid precursor shows the peaks of a hydroxyl group at  $3400\ \text{cm}^{-1}$ , indicating that hydrolysis of an ethoxy moiety occurred. Absorption of the Si-ethoxy bond at  $1136\ \text{cm}^{-1}$  decreased slightly and the new absorption peak of the Si-O-Si band at  $1070\ \text{cm}^{-1}$  increased. This suggests that the formation of the Si-O-Si bond is via the condensation reaction between the hydrolyzed Si-OH and Si-OEt. After curing at  $170\ ^\circ\text{C}$  for 3 h, the peaks of the hydroxyl group at  $3400\ \text{cm}^{-1}$  and the Si-ethoxy bond at  $1136\ \text{cm}^{-1}$  almost disappeared, but the new absorption peak of Si-O-Si at  $1070\ \text{cm}^{-1}$  became

(21) Teng, C. C.; Man, H. T. *Appl. Phys. Lett.* **1990**, *58*, 1743.

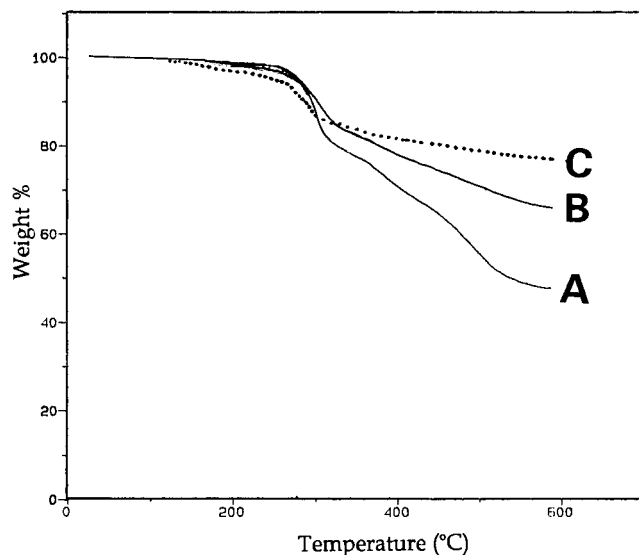
(22) Kang, S. J.; Lee, H. J.; Park, J. T.; Choi, S. K.; Kim, H. K. *Nonlinear Opt.* **1996**, *15*, 277.



**Figure 2.**  $^{29}\text{Si}$  solid-state MAS NMR spectra of the organic/ $\text{SiO}_2$  hybrid material of SG-DANS (1:2:2): (a) a hybrid precursor annealed at  $60^\circ\text{C}$  for 12 h and (b) the organic/ $\text{SiO}_2$  hybrid material cured at  $170^\circ\text{C}$  for 3 h.

stronger. This indicates that the Si–O–Si bond was further formed by the thermal condensation reaction between Si–OH and Si–OEt. Comparing the intensity of the IR spectrum of the respective hydroxyl groups of the homopolymer to that of the copolymer obtained with TEOS reveals that the intensity of the hydroxyl group of the homopolymer is much higher than that of the copolymer. This indicates that the hydroxyl group in the homopolymer remained uncondensed. In other words, the homopolymer could have some difficulty in undergoing the cross-linking reaction between Si–OH and Si–OEt, due to the poor chance of collision between them. This could be explained by the fact that silanol (Si–OH) or ethoxysilane (Si–OEt) groups anchored to the bulky NLO chromophore are not mobile enough to allow reaction between Si–OH and Si–OEt. The addition of TEOS could give a greater chance of cross-linking between Si–OH and Si–OEt, due to the congestion of TEOS between silanol (Si–OH) and ethoxysilane (Si–OEt) groups anchored to the bulky NLO chromophore. Therefore, there are more active sites for the condensation reaction for the copolymer system consisting of large amounts of TEOS, given that the homopolymer has lower degree of polycondensation than the copolymer has.

$^{29}\text{Si}$  MAS NMR spectroscopy was also carried out to monitor the condensation reaction between the dye-attached sol–gel monomer and TEOS. Figure 2 shows the  $^{29}\text{Si}$  MAS NMR spectra of the sol–gel materials. The T species originate from the monomer, where the silicon atom is coordinated by three oxygen atoms. The Q species originate from TEOS, in which the silicon atom is coordinated by four oxygen atoms. There are four classes of T species: the trihydroxy ( $\text{T}^0$ ), dihydroxy ( $\text{T}^1$ ), monohydroxy ( $\text{T}^2$ ), and nonhydroxy ( $\text{T}^3$ ). Q species have five classes as follows: tetrahydroxy ( $\text{Q}^0$ ), trihydroxy ( $\text{Q}^1$ ), dihydroxy ( $\text{Q}^2$ ), monohydroxy ( $\text{Q}^3$ ), and nonhydroxy

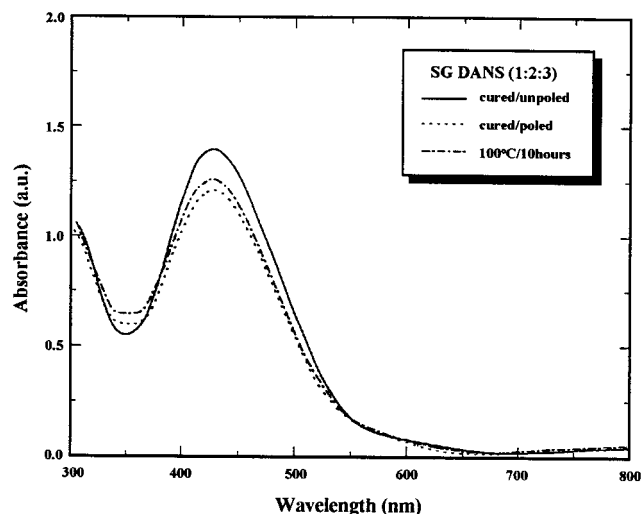


**Figure 3.** TGA curves of the organic/ $\text{SiO}_2$  hybrid materials of SG-DASS: (a) a SG-DASS (1:2:0) cured at  $170^\circ\text{C}$  for 3 h, (b) SG-DASS (1:2:2) cured at  $170^\circ\text{C}$  for 3 h, and (c) SG-DANS (1:2:3) cured at  $170^\circ\text{C}$  for 3 h.

( $\text{Q}^4$ ) states. The  $^{29}\text{Si}$  MAS NMR spectrum of uncured sample (Figure 2a) shows three peaks of T species, due to  $\text{T}^1$  (49.5 ppm),  $\text{T}^2$  (56.6 ppm), and  $\text{T}^3$  (65.1 ppm) units, and also three peaks of Q species, corresponding to  $\text{Q}^1$  (81 ppm),  $\text{Q}^2$  (90.0 ppm),  $\text{Q}^3$  (99.4 ppm) units. After curing of the sample at  $170^\circ\text{C}$  for 3 h, the peaks  $\text{T}^1$ ,  $\text{Q}^1$ , and  $\text{Q}^2$  disappeared and the intensity of the  $\text{T}^3$  (65.1 ppm) and  $\text{Q}^4$  (109.2 ppm) species (fully condensed) increased. These results are consistent with FT-IR data. They indicate that further condensation occurred and the degree of condensation for the silica network increased during the curing process, yielding a highly cross-linked silicon–oxygen polymeric network. This phenomenon is related to the increase of the glass transition temperature ( $T_g$ ) and the dimensional stability of the sol–gel material for copolymers with TEOS.

The thermal properties of the organic/ $\text{SiO}_2$  hybrid materials were examined by thermogravimetric analysis (TGA) and differential scanning calorimeter (DSC). We could not observe clearly the glass transition temperature of the organic/ $\text{SiO}_2$  hybrid material (SG-DANS (1:2:2)) up to  $240^\circ\text{C}$  by DSC. The  $T_g$  of the organic/ $\text{SiO}_2$  hybrid material (SG-DANS (1:2:2)), cured at  $170^\circ\text{C}$  at 3 h, should have higher  $T_g$  than  $150^\circ\text{C}$ , because the organic/ $\text{SiO}_2$  hybrid material (SG-DANS (1:2:2)) has a high cross-linking density in the  $^{29}\text{Si}$  MAS NMR spectra. A similar result was obtained from the temporal stability study of the poled hybrid films, in which 80% of the  $r_{33}$  signal remained after heating even at  $150^\circ\text{C}$  for 3 h (see the next section).

The thermal stability of the resulting hybrid material was evaluated by TGA under a nitrogen atmosphere (see Figure 3). The TGA data exhibits the initial decomposition temperature at 265, 273,  $278^\circ\text{C}$  for the organic/ $\text{SiO}_2$  hybrid materials of SG-DANS (1:2:0), (1:2:2), (1:2:3), which contain 100, 50, and 25 wt % of NLO chromophore-containing sol–gel monomer in the hybrid, respectively (see Figure 3). The organic/ $\text{SiO}_2$  hybrid material of SG-DANS (1:2:3) exhibits the greatest thermal stability among them. These organic/ $\text{SiO}_2$  hybrid materials exhibit better thermal stability with



**Figure 4.** The absorption spectra of the SG-DANS (1:2:3) film before corona poling, after corona poling, and after keeping at 100 °C for 100 h.

greater TEOS content, because the degree of polycondensation was higher with greater TEOS content than with less. This result is in agreement with FT-IR and  $^{29}\text{Si}$  MAS NMR results.

Also, after curing/poling at 170 °C for 3 h, red-colored, organic/SiO<sub>2</sub> hybrid films with good optical quality were obtained. This observation implies that the organic/SiO<sub>2</sub> hybrid films did not have any macroscopic phase separation during the curing/poling process. This is very important for device applications to reduce the optical loss due to scattering. To elucidate the relationship between structure and transparency, we carried out an atomic microprobe analysis by scanning electronic microscopy (SEM). The surface of the film did not have visible cracks and the macrophase separation did not occur in any samples after the curing or corona poling process. The SEM photograph showed no microphase separation on the micron scale in any of the hybrid polymer films (see the Supporting Information). To analyze the morphology of the organic/SiO<sub>2</sub> hybrid films in more detail, the surface properties of the organic/SiO<sub>2</sub> hybrid films were examined by atomic force microscopy (AFM). Seiko SPA-300 atomic force microscopy equipped with an SPI-3700 controller was used to observe the surface morphology of the films. The cantilever probe (Olympus) had a 100 nm long pyramidal tip (Si<sub>3</sub>N<sub>4</sub>) and its force constant was 0.09 N/m. Microphase separation on the nanometer scale was not detected (see the Supporting Information).

We also investigated the morphology of these organic/SiO<sub>2</sub> hybrid materials by X-ray diffractometry. In general, the X-ray diffraction pattern of an amorphous polymer is broad and the ratio of the half-height width to diffraction angle ( $2\theta/2\theta$ ) is greater than 0.35, while the diffraction peaks of crystalline materials are sharp and their values of  $2\theta/2\theta$  are smaller than 0.05. The values of the diffraction angle of the present hybrid materials are greater than 0.55, indicating that all of the hybrid materials are amorphous. Thus, X-ray diffraction showed that the hybrid materials had an amorphous structure. The amorphous property of a polymeric film is important so that light propagates through the material without being scattered.

**Table 1. Physical Properties, Linear and Nonlinear Optical Properties for the Organic/SiO<sub>2</sub> Hybrid Materials Based on SG-DANS**

sample	$\lambda_{\text{max}}$ (nm)	wt. % dye in the matrix	$T_d^a$ (°C)	$n^b$ (1.3 $\mu\text{m}$ )	$r_{33}^c$ (pm/V) (1.3 $\mu\text{m}$ )
SG-DANS (1:2:0) <sup>d</sup>	446	55	265	1.608	3.7
SG-DANS (1:2:1)	443	50	272	1.592	12.4
SG-DANS (1:2:2)	443	42	273	1.5636	7.8
SG-DANS (1:2:3) <sup>e</sup>	441	26	278	1.560	9.1

<sup>a</sup> Decomposition temperature of NLO dye incorporated in silica network. <sup>b</sup> Indices of refraction were determined from a waveguide experiment at the wavelength of 1.3  $\mu\text{m}$ . <sup>c</sup> Electrooptic coefficient was measured at the wavelength of 1.3  $\mu\text{m}$ . <sup>d</sup> Molar ratio of DANS diol, IP-TriEOS, and TEOS. <sup>e</sup> Cracking of film is prone to happen because of the stress on the film induced by contraction during condensation reaction.

**Linear and Nonlinear Optical Properties of the Hybrid Film.** The absorption spectrum of the films was measured with a Shimadzu UV-3101PC spectrophotometer. Figure 4 shows the absorption spectra of SG-DANS (1:2:3) hybrid film before and after corona poling and of poled SG-DANS (1:2:3) hybrid film kept at 100 °C for 100 h. For the unpoled film, the absorption peak appears at  $\lambda_{\text{max}} = 426$  nm. After corona poling at 170 °C for 30 min, the peak intensity was reduced. Its reduction is due to the fact that the molecular dipoles were aligned along the direction of the applied field. When the film was maintained at 100 °C for 10 h, the absorption peak of the film increased again, indicating that some randomization of the aligned NLO molecules by thermal movement occurred.

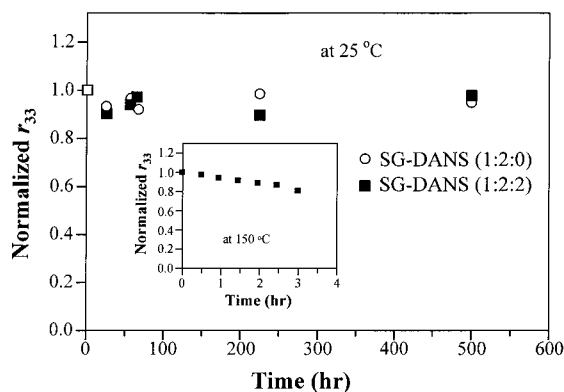
The refractive indices for the unpoled films were determined by using a prism-coupling method from the coupling angles of the TE modes in the slab waveguide configuration. The laser diode light was coupled in to and out of the polymer films spin-coated on cover glass with a gadolinium gallium garnet (GGG) prism. In this case, the cover glass acts as the substrate with a lower refractive index than that of the polymer film. As a result, the hybrid film forms a planar waveguide, since the light is guided along the polymer film between the air and the substrate. The beam is totally reflected except for the coupling conditions to waveguiding modes which determine the guiding mode angles. A calculation based on the theory given in a cited reference<sup>23</sup> was used to determine the film's refractive index and thickness from the measured guiding mode angles. Table 1 summarizes the wavelength of maximum visible absorption ( $\lambda_{\text{max}}$ ) and the refractive index measured at the wavelength of 1.3  $\mu\text{m}$  for the unpoled hybrid films. It is observed that the refractive index of the SG-DANS (1:2:0) film gave higher values than that of the SG-DANS (1:2:3) film having smaller NLO chromophore content.

The electro-optic coefficients of hybrid films poled by a corona discharge technique were measured at a wavelength of 1.3  $\mu\text{m}$  using the simple reflection method.<sup>21</sup> Table 1 presents the electro-optic coefficients of the SG-DANS hybrid films. The poled/cured hybrid films of SG-DANS (1:2:0), (1:2:1), (1:2:2), (1:2:3) have  $r_{33}$  values of 3.7, 12.4, 7.8, and 9.1 pm/V, respectively.

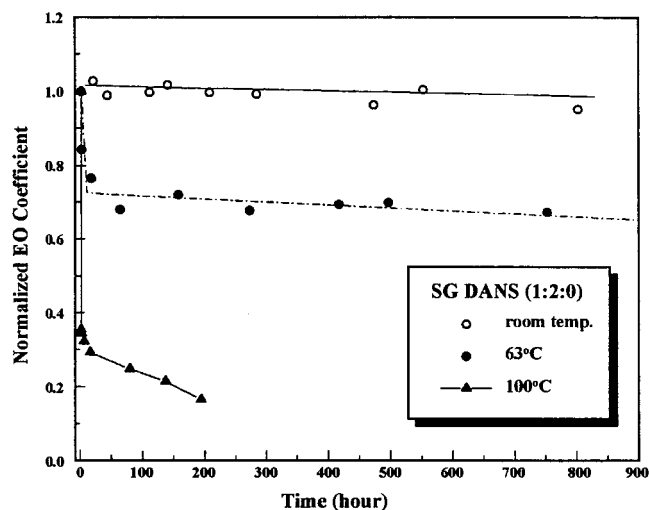
To evaluate the temporal and thermal stability of the poled hybrid films, we measured the electro-optic coef-

(23) Page, R. H.; Jurishc, M. C.; Reck, B.; Sen, A.; Twieg, R. J.; Swalen, J. D.; Bjorklund, G. C.; Willson, C. G. *J. Opt. Soc. Am. B* **1990**, *7*, 1239.





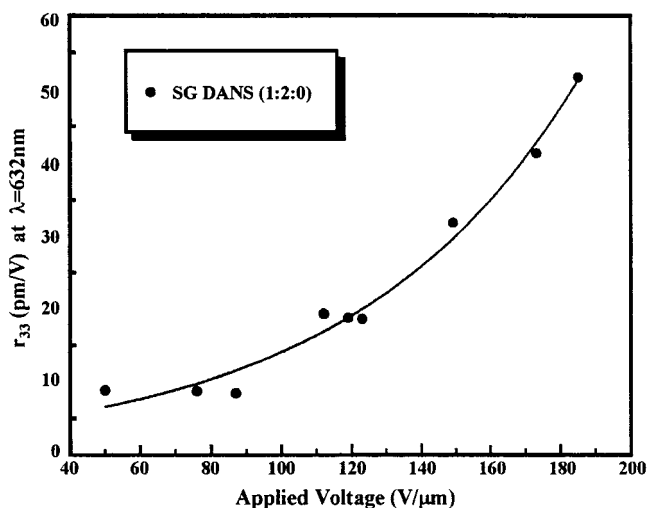
**Figure 5.** Temporal stability of the electro-optic coefficient  $r_{33}$  for the SG-DANS (1:2:0) film and the SG-DANS (1:2:2) film poled/cured at 170 °C for 3 h.



**Figure 6.** Temporal and thermal stability of the electro-optic coefficient  $r_{33}$  for the SG-DANS (1:2:0) at room temperature and 63 and 100 °C.

cient as a function of time (hours) at different temperatures. It was observed that the EO coefficient did not decay at room temperature after the storage of 20 days (see Figure 5). This result indicates that the orientation of the NLO chromophores in the SG-DANS (1:2:2) hybrid film shows no significant relaxation under ambient conditions within 20 days after poling. Also, the thermal stability of the EO coefficient of the SG-DANS (1:2:2) hybrid film was investigated at elevated temperature. The hybrid film shows that 80% of the initial  $r_{33}$  signal remained after heating the poled film at 150 °C for 3 h. It can be deduced that the  $T_g$  of film must be higher than 150 °C, even though the  $T_g$  was not detected by DSC.

Also, Figure 6 shows the temporal and thermal stability of the electro-optic coefficient  $r_{33}$  for the SG-DANS (1:2:0) hybrid film at room temperature and 63 and 100 °C. The film was corona poled with an applied voltage of 6 kV at 230 °C for 1 h. At room temperature, the film retained about 95% of its initial  $r_{33}$  value after 800 h. At 63 °C, the EO coefficient dropped rapidly to 70% of its initial  $r_{33}$  value within 100 h and then the rate of decrease was reduced. The film retained 65% of its initial  $r_{33}$  value after 800 h. At 100 °C, the  $r_{33}$  value decreased more rapidly. Comparing the two different types of film, the SG-DANS (1:2:2) hybrid film showed both better temporal and thermal stability of the electric



**Figure 7.** Change of the electro-optic coefficient  $r_{33}$  for the SG-DANS (1:2:0) as a function of the applied voltage.

field induced alignment than the SG-DANS (1:2:0) film. The enhancement of the temporal and thermal stability in the SG-DANS (1:2:2) hybrid film may be due to the higher network density of the silica matrix obtained by adding TEOS as a cross-linker, which is in agreement with other analytic results.

Using a dc contact poling process, the relationship between the electro-optic coefficients and the applied voltage was investigated, for the first time as far as we know. The SG-DANS (1:2:0) hybrid film and the SG-DANS (1:2:2) film were used in this experiment. For the SG-DANS (1:2:3) hybrid film, a large poling current (several tens of microampere) was observed, which cause severe degradation of the electrode and the film. The relationship between the electro-optic coefficient and the applied voltages for the SG-DANS (1:2:0) hybrid film poled at 150 °C for 30 min under various applied voltages is shown in Figure 7. The EO coefficient increased exponentially with the applied voltage. The largest  $r_{33}$  value obtained for this film at a wavelength of 0.633 μm was 52 pm/V at an applied electric field of 130 V/μm. At a wavelength of 1.3 μm, the largest  $r_{33}$  value obtained was 16 pm/V.

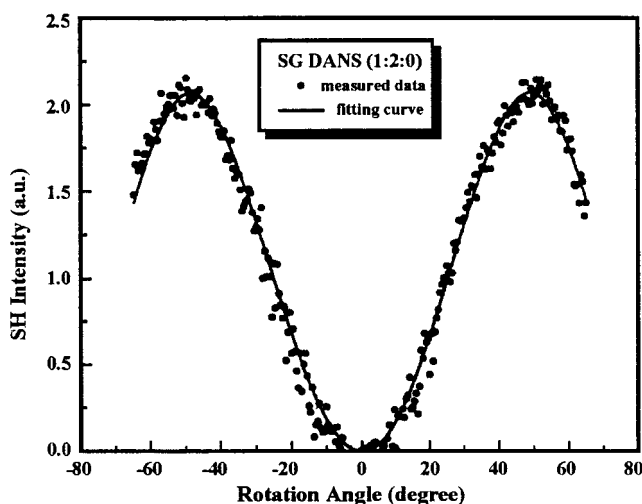
Table 2 summarizes the electro-optic coefficients of the SG-DANS (1:2:2) hybrid film measured at the wavelength of 1.3 μm under different prebaking and dc contact poling conditions. For SG-DANS (1:2:2) hybrid film prebaked at 180 °C for different periods of time, it was observed that the  $r_{33}$  value was not much affected by the poling temperature. As the applied voltage increased, the EO coefficient increased linearly. The largest  $r_{33}$  value in the present study was 7.36 pm/V for the SG-DANS (1:2:2) hybrid film when the applied electric field of 130 V/μm. Our results indicate that the corona poling process is more effective than the dc contact poling.

We also measured the second-order nonlinear optical coefficient  $d_{31}$  of the SG-DANS (1:2:0) hybrid film by the Maker fringe technique using 1064 nm as the fundamental radiation, since the absorption at the second-harmonic wavelength of 532 nm is too large to be ignored. The equation derived by Herman and

**Table 2. Electrooptic Coefficients of the SG-DANS (1:2:2) Film Measured at the Wavelength of 1.3  $\mu\text{m}$  at Different Prebaking and Direct-Current Contact Poling Conditions**

sample no.	soft bake	poling condn	poling current ( $\mu\text{A}$ )	applied voltage ( $\text{V}/\mu\text{m}$ ) <sup>a</sup>	$I_c$ (mV)	$I_m$ (A point) ( $\mu\text{V}$ )	$I_m$ (B point) ( $\mu\text{V}$ )	$V_m$ (V)	$r_{33}$ (pm/V)
1	180 °C/20 min	130 °C/30 min		112	253.3	31.4	16	6.364	6.76
2	180 °C/30 min	160 °C/30 min		104	247.7	14.7	14.0	6.364	4.18
3	180 °C/20 min	160 °C/30 min	4.4	102	251.1	17.1	21.0	6.364	5.48
4	180 °C/40 min	160 °C/30 min	0.7	96	237.2	13.1	13.2	6.364	4.00
5	180 °C/2 h	160 °C/30 min	1.2	99	249.7	22.0	18.5	6.364	5.86
6	180 °C/20 min	160 °C/30 min		117	260.8	18.7	22.2	6.364	5.66
7	180 °C/20 min	150 °C/30 min	11	97	166.4	22.5	2.0	6.364	5.32
8	180 °C/20 min	150 °C/30 min	2.6	130	248.7	23.1	27.6	6.364	7.36
9	180 °C/20 min	150 °C/30 min	0.6	84	202.5	15.1	8.5	6.364	4.21
10	180 °C/20 min	150 °C/30 min	1.4	107	132.4	9.38	12.7	6.364	6.02
11	180 °C/30 min	160 °C/2 h		86	250.0	17.5	15.4	6.364	4.75
12	180 °C/40 min	180 °C/30 min	1.3	98	245.6	15.8	15.2	6.364	4.56

<sup>a</sup> Starting temperature, 65 °C; temperature ramp, 10 °C/min for increase and -5 °C/min for decrease; voltage off at 75 °C.

**Figure 8.** Maker fringe pattern of a corona-poled SG-DANS (1:2:0) film and a fitting curve.

Hayden, which takes into consideration the absorption of the material, must be used for the calculation.<sup>24</sup> The thickness of the film was 0.75  $\mu\text{m}$ , and the absorption coefficient at a wavelength of 532 nm was measured to be  $\alpha = 1.29 \mu\text{m}^{-1}$ . The refractive index was 1.83 at a wavelength of 532 nm and 1.61 at a wavelength of 1064 nm. The input beam was s-polarized and the output second-harmonic intensity, after passing through a band-pass filter and a p-polarizer, was detected by a photomultiplier tube.

Figure 8 shows the Maker fringe pattern of the poled film. The solid line is a fitting curve. From these data fit, a  $d_{31}$  value of 72 pm/V was obtained. Since the relationship  $d_{33} \approx 3d_{13}$  holds in polymer systems,<sup>25</sup> the  $d_{33}$  value is supposed to be about 216 pm/V. To compare the second-order nonlinear coefficient and the electro-optic coefficient, the  $r_{33}$  value for the same sample was measured by a simple reflection method. The  $r_{33}$  value measured was 35 pm/V at 632 nm and 12 pm/V at 1.3  $\mu\text{m}$  wavelength. It should be noted that there is a big discrepancy between the  $d_{33}$  value and the  $r_{33}$  value for the same hybrid materials, due to some resonant enhancement at a wavelength of 532 nm. A DANS NLO chromophore has the UV-vis absorption tailing at a wavelength of 532 nm, which corresponds to the two-photon absorption wavelength of the measuring wavelength of 1064 nm. A much higher  $d_{33}$  value is yielded when the  $d_{33}$  value and the  $r_{33}$  value were measured at the wavelength of 1064 and 1300 nm, respectively.

**Table 3. Physical Properties, Linear and Nonlinear Optical Properties for the Organic/SiO<sub>2</sub> Hybrid Materials Based on SG-DASS II and SG-DASS III**

sample	$\lambda_{\text{max}}$ (nm)	$T_d$ (°C)	$n^b$ (1.3 $\mu\text{m}$ )	$r_{33}$ , pm/V <sup>c</sup> (1.3 $\mu\text{m}$ )
SG-DASS II (1:2:0)	386	268	1.569	4.7
SG-DASS II (1:2:2)	384	275	1.537	7.6
SG-DASS III (1:2:0)	389	266	1.568	2.7
SG-DASS III (1:2:3)	387	274	1.522	4.3

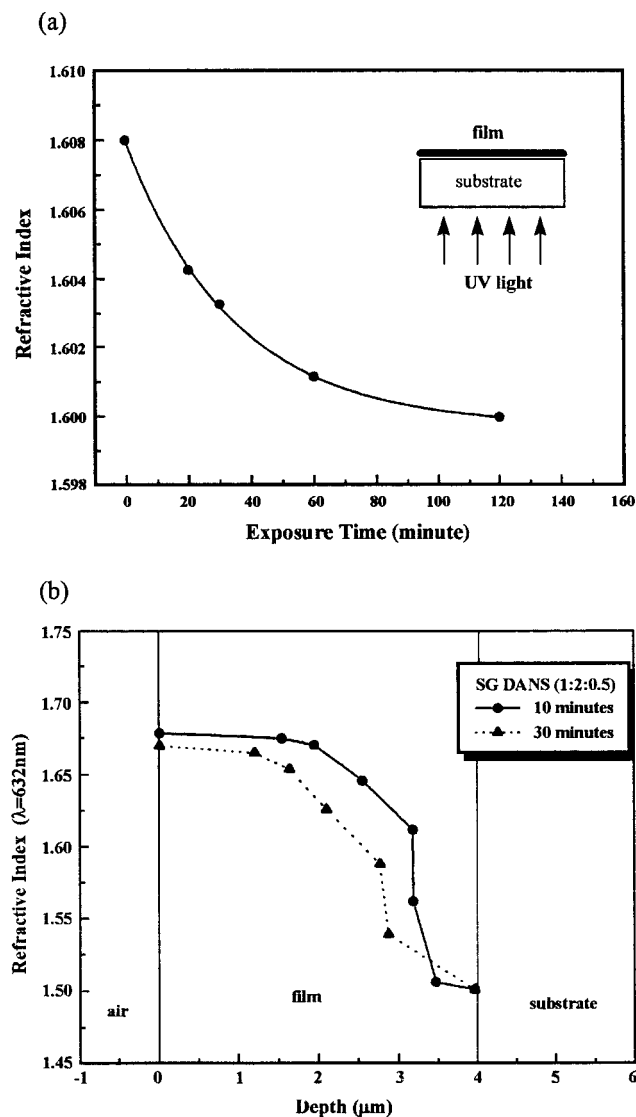
<sup>a</sup> Decomposition temperature of NLO dye incorporated in silica network. <sup>b</sup> Indices of refraction were determined from waveguide experiment at the wavelength of 1.3  $\mu\text{m}$ . <sup>c</sup> Electrooptic coefficient was measured at the wavelength of 1.3  $\mu\text{m}$ . <sup>d</sup> Molar ratio of DASS diol, IP-TriEOS, and TEOS. <sup>e</sup> Molar ratio of DASS triol, IP-TriEOS, and TEOS.

Also, some physical properties and linear and nonlinear optical properties for the organic/SiO<sub>2</sub> hybrid materials based on SG-DASS II and SG-DANS III are summarized in Table 3. The electro-optic coefficients of the cure/poled hybrid films obtained from SG-DASS II hybrid film have  $r_{33}$  values of 4.7 and 7.6 pm/V for the SG-DASS II (1:2:0) hybrid film and the SG-DASS II (1:2:2) hybrid film, respectively. The temporal stability of the EO coefficients for the SG-DASS II was not measured. However, it may be deduced that the temporal stability of the SG-DASS II hybrid films may be better than that of the SG-DANS, since the DASS chromophore, having a long hexylsulfonyl moiety, has more restrictions to its motion. It was assumed that the degree of cross-linking density is similar to that of the SG-DANS hybrid film, due to the similar preparations of the SG-DANS hybrid films. For the trifunctionalized SG-DASS III hybrid film, obtained similarly to the preparation of the SG-DANS hybrid film, the electro-optics coefficients of the cure/poled hybrid films have  $r_{33}$  values of 2.7 and 4.3 pm/V for the SG-DASS III (1:2:0) and the SG-DASS III (1:2:2) hybrid films, respectively. The low  $r_{33}$  value obtained is attributed to the difficulty in aligning the dipole moment of the DASS chromophore, due to a high-cross-linking density, where the DASS chromophore was fixed and anchored at three end groups to silica networks to restrict its free rotation.

To provide vertical confinement of light, a buried channel waveguide requires upper and lower cladding layers, composed of lower index materials with a middle layer of higher index material. To provide horizontal

(25) Prasad, P. N.; Williams, D. J. *Introduction to Nonlinear Optical Effect in Molecules and Polymers*; Wiley: NY, 1991; p 66.





**Figure 9.** (a) Change of the refractive index as a function of an exposure time from a large area UV light illuminator with the spectral range of 320 to 450 nm, and (b) distribution of the refractive index inside the film calculated by using inverse WKB approximation.

confinement, also, when fabricating a channel waveguide, the difference of refractive index between core and cladding is required to be about 0.01 in order to minimize the coupling loss. This small refractive index difference can be easily realized by a photobleaching effect in NLO poled polymers. The photobleaching effect is a kind of photochemical reaction, such as cis–trans isomerization and photooxidation of NLO chromophores.<sup>26</sup> The refractive index change of SG DANS (1:2:0) film was measured as a function of exposure time. As an UV light source, a large area illuminator (Oriel Inc.) with the spectral range between 320 and 450 nm was used. The intensity of the UV light was 55 mW/cm<sup>2</sup> and the film was illuminated from the substrate side. The refractive indices were measured by the prism coupling method. The procedure becomes very simple and the scattering loss can be reduced greatly as compared with

the etching method, when the photobleaching effect is used in fabricating the channel waveguide.<sup>27</sup>

Figure 9a shows a preliminary result for the refractive index change as a function of photobleaching time for SG-DANS (1:2:0). The indices were calculated on the assumption that the photobleached film had uniform index change everywhere inside the film. The refractive index decreased with time and the curve is well-fitted by an exponential function with a single decay time,  $\tau = 30$  min. With an exposure time of 1 h, an index change of 0.006 could be obtained. But, in fact, when the film is bleached, the refractive index change varies with the depth, so there is an index distribution curve inside the film. This index distribution can be calculated by inverse WKB approximation<sup>28</sup> using data measured from a prism coupling method (Figure 9b).<sup>26</sup> This photobleaching technique can give the channel patterning.

Using a photobleaching method, a single-mode channel waveguide was fabricated.<sup>29</sup> The geometry of the single-mode channel waveguide, fabricated on the silicon wafer, was designed by Marcatili's method<sup>30</sup> so that the guiding area of  $3.3 \times 5 \mu\text{m}^2$  could support a single mode. The length of the waveguide was 5 mm. The lower cladding and the active core layer were made of the SG-DANS (1:2:3) film and the SG-DANS (1:2:0.5) film, respectively, and AZ4562 positive photoresist was used for the upper cladding. A channel waveguide was achieved by illuminating the cladding area with the intense UV light of a 350 W halogen lamp for 2 h, except for the core region. The photobleaching effect reduced the magnitude of the refractive index by 0.009. The refractive indices of the lower cladding, core, and upper cladding at 1.3  $\mu\text{m}$  wavelength were measured to be 1.59, 1.609, and 1.595, respectively (see Figure 10a). A TM polarized laser beam of 1.3  $\mu\text{m}$  wavelength entered one end face of the waveguide and the output near-field pattern was recorded with a charge-coupled device (CCD) camera (Figure 10b). The fundamental single mode was observed.

Another major issue with real applications of poled NLO polymers is optical propagation loss (OPL). The OPL of the organic/silica hybrid film was measured by the method of analyzing the guided streak of laser light.<sup>31</sup> A SG-DANS (1:2:0.5) film of  $\sim 2 \mu\text{m}$  thickness was spin-coated on a clean glass slide and cured at 180 °C for 30 min. A TE polarized laser beam of 1.3  $\mu\text{m}$  wavelength was coupled into the film by the prism coupling method and the streak image of the guiding mode was detected by CCD camera. The optical loss was determined from the scattered signal as the beam propagated through the planar waveguide. The OPL was measured to be less than 1 dB/cm. Furthermore, using the hybrid material, a Mach–Zender modulator is being fabricated and characterized.<sup>32</sup> The optical loss will also be determined

(27) Lee, M. H.; Lee, H. J.; Han, S. G.; Kim, H. Y.; Kim, K. H.; Kang, S. Y. *Solid Thin Film* **1997**, *303*, 287.

(28) Shite, J. M.; Heidrich, P. F. *Appl. Opt.* **1976**, *15*, 151.

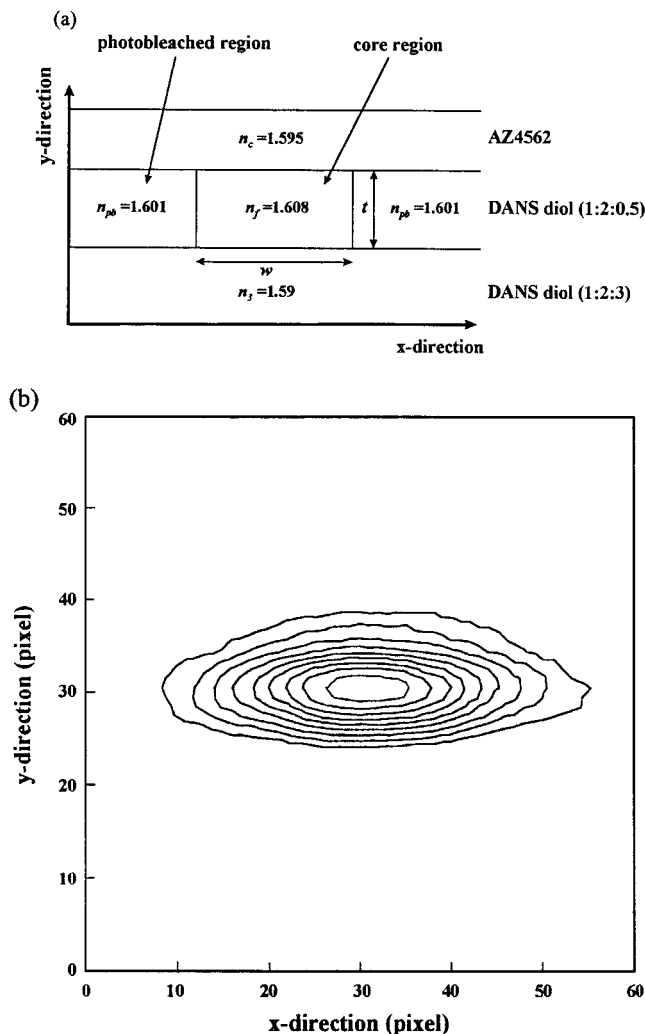
(29) Min, Y. H.; Yoon, C. S.; Kim, H. K.; Kang, S. J. *J. Kor. Phys. Soc.* **1997**, *31*, 443.

(30) Marcatili, J. E. A. *Bell Syst. Technol. J.* **1969**, *48*, 2071.

(31) Kowalczyk, T. C.; Kosc, T.; Singer, K. D.; Cahill, P. A.; Seager, C. H.; Meihardt, M. B.; Beuhler, A. J.; Wargowski, D. A. *J. Appl. Phys.* **1994**, *76*, 2505.

(32) Min, Y. H.; Yoon, C. S.; Kim, H. K. *Adv. Mater.* To be submitted.

(26) Dieme, M. B. J.; Suyten, F. M. M.; Trommel, E. S.; McDonach, A.; Copeland, M.; Jenneskens, L. W.; Horsthius, W. H. G. *Electron. Lett.* **1990**, *26*, 380.



**Figure 10.** (a) Cross sectional structure of a channel waveguide and (b) the mode profile of the output near-field pattern detected by CCD camera.

### Conclusions

Thermally stable second-order NLO polymeric materials were synthesized by the coupling reaction of 3-isocyanatopropyltriethoxysilane with the corresponding functionalized NLO chromophores in DMAc. The dye-attached sol-gel monomer (ormosils) was homopolymerized and copolymerized with TEOS by hydrolysis

and polycondensation in the presence of a slight excess of acidified water (pH 3). The hybrid precursors were spin-coated on the various substrates, such as ITO glass and NaCl disks. Hybrid films were further polycondensed by curing at 170 °C for 3 h. The cured hybrid materials existed in monohydroxy ( $T^3$ ,  $Q^3$ ) and nonhydroxy ( $T^3$ ,  $Q^4$ ) states after curing at 170 °C for 3 h, indicating the formation of a highly cross-linked silicon-oxygen polymeric network. All of the cured organic/ $SiO_2$  hybrid films are transparent. A phase separation was not detected by SEM. The AFM photograph showed that the films have good surface flatness. The organic/ $SiO_2$  hybrid materials were quite stable at elevated temperatures above 250 °C. The hybrid films were poled by corona discharge technique or dc contact electrode under the different conditions. The values of electro-optic coefficients for the organic/ $SiO_2$  hybrid materials were in the range of 3.7–16 pm/V at a wavelength of 1.3  $\mu\text{m}$ , depending on dye-attached sol-gel monomers and poling conditions. The SG-DANS (1:2:2) film shows excellent temporal stability. The  $r_{33}$  signal remained 80% of its initial value after heating even at 150 °C for 3 h. By using the dc contact poling method, a large EO coefficient of  $r_{33} = 16$  pm/V at 1.3  $\mu\text{m}$  wavelength was obtained. The relationship between the EO coefficient and the applied poling voltage was investigated. Also, the second-order nonlinear optical coefficient  $d_{31}$  of 72 pm/V for the SG-DANS (1:2:0) hybrid film measured by the Maker fringe technique was obtained. The refractive index was decreased after photobleaching. Using the hybrid film, a single-mode channel waveguide was fabricated by the photobleaching method. The mode pattern confirmed that the channel waveguide was single-mode, and the optical propagation loss was measured to be less than 1 dB/cm.

**Acknowledgment.** This research was financially supported from the Korean Science and Engineering Foundation under the Contact No. of 951-0305-015-1.

**Supporting Information Available:** (a) A SEM photograph and (b) a AFM photograph for the organic/ $SiO_2$  hybrid material of SG-DANS (1:2:2) cured at 170 °C for 3 h. This material is available free of charge via the Internet at <http://pubs.acs.org>.

CM980652A